

Context-aware Automatic Music Transcription

Federico Simonetta, Stavros Ntalampiras, Federico Avanzini

LIM — Music Informatics Laboratory

Department of Computer Science

University of Milan

Email: {name.surname}@unimi.it

Abstract—This paper presents an Automatic Music Transcription system that incorporates context-related information. Motivated by the state-of-art psychological research, we propose a methodology boosting the accuracy of AMT systems by modeling the adaptations that performers apply to successfully convey their interpretation in any acoustical context. In this work, we show that exploiting the knowledge of the source acoustical context allows reducing the error related to the inference of MIDI velocity. The proposed model structure first extracts the interpretation features and then applies the modeled performer adaptations. Interestingly, such a methodology is extensible in a straightforward way since only slight efforts are required to train completely context-aware AMT models.

Index Terms—Music, Transcription, Music Information Processing, Neural Networks, Deep Learning, Non-negative Matrix Factorization

I. INTRODUCTION

Automatic Music Transcription (AMT) consists in the analysis of music audio recordings to discover semantically meaningful events, such as notes, instruments and chords. Two main methodologies for AMT exist, i.e. Non-negative Matrix Factorization (NMF) and Deep Learning (DL) (for a thorough review see [1]). During the last 4 years, DL has tremendously advanced the state-of-art of AMT, especially for piano music recordings [2]–[4]. Nonetheless, no attention has been placed on the influence of the environment acoustics on the AMT output.

Various evidence exist proving the influence of the room acoustics on the musician. Different research groups focused their efforts in the understanding of why and how music performers adapt their way of playing to the surrounding acoustics. Analyzed instruments include strings, wind instruments, and piano. All existing studies are directed towards the understanding of the factors characterizing room acoustics and never face the problem from the audio processing perspective [5].

The contribution of the present paper is an attempt to exploit such adaptation phenomena to increase AMT accuracy. One previous work faced a similar problem, but tried to simulate the adaptation phenomenon applied by performers while knowing both the original and destination context [6]. The long-term use-case scenario that motivates the present work, instead, is an audio resynthesis application that allows musicians to achieve studio-quality music recordings with cheap microphones, regardless of the acoustical environment of the source recording. Consequently, we seek the artistic elements that constitute the

expressive intention of the performance. The objective is the rendering of such elements in a new known context – e.g. a virtual instrument. As in a previous work [5], we name these elements “interpretation” while we refer to the actual rendering with “performance”. As it emerges from the current discussion, the performance depends on the acoustical environment where it happens, while the interpretation is independent from it. Such distinction is discussed in more depth in [5].

In this paper, we propose an extensible methodology to assess the benefit coming from context-aware AMT systems. We perform thorough tests with different DL models and demonstrate that context-aware strategies are generally outperforming the traditional context-unaware AMT. Targeting at full reproducibility of the conducted experiments, the implementation is available online¹.

II. EXPERIMENT OVERVIEW

Instead of collecting a new ad-hoc dataset, we leverage the existing datasets for AMT by resynthesizing the various performances in multiple artificial contexts. In this setting, a single performance rendered in two different contexts without any kind of adaptation generates two different audio with two different perceivable interpretations [5]. Thus, the same MIDI notes synthesized in different contexts without any type of adaptation should be considered as generated from different interpretations, even if they have the same underlying MIDI data. Following this idea, we used the MIDI ground-truth data to resynthesize the Maestro dataset [2] in manifold artificial contexts and we explored the way the inference of MIDI parameters can be optimized.

We designed an ad-hoc AMT model for estimating the performance parameters. Since our aim is to understand whether the performance transcription error can be reduced by considering the acoustical context, we focus on performance parameter estimation in a controlled setting where note timings are known.

In realizing an extensible AMT method, we use the perfectly aligned MIDI files recorded by the Disklavier which are available in the Maestro dataset to inform the transcription process. In a real-world scenario, a precise alignment of a score can be obtained using the Audio-to-score method presented in our previous work [7]. We applied Non-negative Matrix Factorization (NMF) [8] to perform a source-separation of each single key of the piano and then analyzed the spectral representation of each source-separated note. Namely, we compute the MFCCs

¹<https://limunimi.github.io/MIA/>

characterizing timbral aspects that are connected to the note velocity due to the piano acoustics [9] and are independent of the non-linear amplitude distortions of the microphones [10], [11]. Then, we employ a Convolutional Neural Network (CNN) model to infer the velocity of each note.

The CNN model is split in two parts as follows:

- 1) the “encoder”, which infers the interpretation and takes as input the note-separated spectrogram with size 13×30 and one channel;
- 2) the “performer”, which adapts the interpretation to the given source context by taking the latent output of the encoder and computing the estimated velocity in the source acoustical context.

Given a single MIDI data synthesized in various contexts, the encoder should infer the interpretation in a way that is dependent on the source context, while the performer should predict the same ground-truth data for all contexts.

Since we aim at showing that knowing the source context is beneficial regardless the approximation error, we repeat the experiments with various types of function. More precisely, we define a set of hyper-parameters that determine the shape of the neural network model and then perform a grid-search to explore how the error changes when different model structures are used for the estimation.

Furthermore, we considered various strategies for context-awareness. More specifically:

- 1) the performer can be the same for every context, i.e. context-independent, or it can be context-specific, meaning that in the model there is a different performer for each context;
- 2) the latent space found by the encoder should be context-aware, meaning that it should still include the information required for identifying the input context; as such, it is interesting to understand if enforcing this property facilitates the learning process.

The implementation of the first variable consists in building one performer per context or one performer for every context. As regards to the second variable, we add an additional branch to the model to classify the input context based on the encoder output; this branch works as a learnable loss function that separates the latent space according to the input context.

We compared the 4 different strategies resulting by the combinations of the above-mentioned 2 boolean variables, i.e.

- **False-False:** one single performer and no context classification – this case corresponds to context-unaware AMT;
- **True-False:** one performer per context without using a context classifier;
- **False-True:** one single performer with context classifier;
- **True-True:** one performer per context and context classification.

All four strategies were tested for each point in the hyper-parameter space, resulting in a highly computationally demanding experiment. We thoroughly tested 36 different model shapes, each with 4 different training strategies, summing up to 144 trained models.

Table I
SUMMARY OF THE MAIN CHARACTERISTICS OF THE 6 PRESETS USED FOR RESYNTHESIZING THE MAESTRO [12] DATASET.

ID	Velocity Map	Reverb	Instrument
0	Linear	Jazz Studio	Steinway B Prelude
1	Logarithmic	Jazz Studio	Steinway B Prelude
2	Logarithmic	Cathedral	Steinway B Prelude
3	Linear	Jazz Studio	Grotrian Cabaret
4	Logarithmic	Jazz Studio	Grotrian Cabaret
5	Logarithmic	Cathedral	Grotrian Cabaret

III. DATASET

This section describes the data creation process facilitating the proposed experiment.

A. Resynthesis

We designed an experiment based on the resynthesis of existing datasets. To this end, we developed `pycarla`², a Python module that leverages the excellent `Carla`³ plugin host to synthesize MIDI messages both in real-time and offline using the major audio plugin formats – such as VST, AU, LV2, LADSPA, DSSI, SF2, SFZ.

We used 6 different presets for the physically modeled virtual piano by Pianoteq, kindly provided for research purposes by Modartt⁴. Table I summarize the main characteristics of each preset.

B. Clustering

The source dataset was Maestro [12] and was used as provided by ASMD library [13]. The Maestro dataset was selected using the ASMD Python API; then, *train*, *validation*, and *test* splits were partitioned in 6 different subsets, each associated to one of the presets in Table I, for a total of $6 \times 3 = 18$ subsets. From 18 subsets, 6 sets were generated by unifying subsets associated to the same preset, so that each set was still split in *train*, *validation*, and *test* sets. Each generated set was resynthesized and saved to a new ASMD definition file.

The 6 new subsets in each split were chosen as follows. First, one split at a time among the already defined *train*, *validation*, and *test* was selected. Supposing that the chosen split has cardinality K , C clusters were created with $C = \lfloor K/6 + 1 \rfloor$ and a target cardinality $t = 6$ was set. Then, a redistribution policy is applied to the points of the clusters: for each cluster with cardinality $< t$ – a “poor” cluster – we look for the point nearest to that cluster’s centroid and belonging to a cluster with cardinality $> t$ – a rich cluster – and move that point to the poorer cluster. The redistribution stops when all clusters have cardinality $\geq t$. Since the redistribution algorithm moves points from rich clusters to the poor ones, we named it “Robin Hood” redistribution policy. Having obtained C clusters each with 6 samples, we partitioned the chosen split in 6 subsets as follows:

- 1) we randomized the order of subsets and clusters

²<https://web.archive.org/web/20211213132835/https://pypi.org/project/pycarla/>

³<https://web.archive.org/web/20211205195725/https://kx.studio/Applications:Carla>

⁴<https://web.archive.org/web/20211112075858/https://www.modartt.com/>

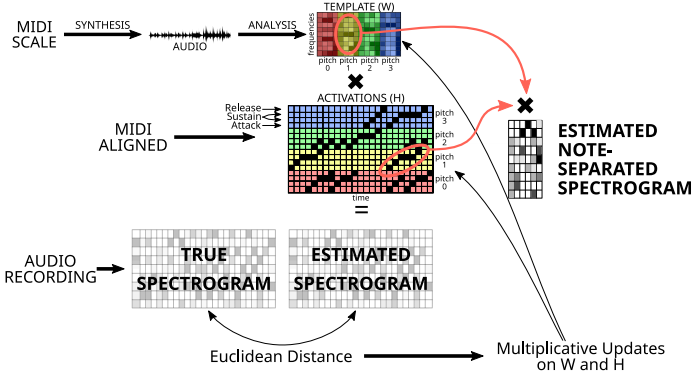


Figure 1. The entire NMF workflow. First, the initial template and activation matrices are computed. Then, the Euclidean distance between the estimated and the true spectrograms is used to multiplicatively update both the template and the activation matrix. Finally, only the relevant part of the template and activations are used for estimating the note-separated spectrogram. For simplicity, 4 columns are used to represent each note while during the experiments, we considered 30.

- 2) we selected one point from each cluster using a random uniform distribution and assigned it to one of the 6 subsets
- 3) we did the same for the other 5 subsets
- 4) we restarted from point 2 until every point is assigned to a cluster.

Details about the clustering procedures are provided in the accompanying website.

IV. NOTE-SEPARATION

NMF has largely been used for score-informed AMT [5], [10], [14], [15] and our application is mainly based on the existing literature. Using NMF, a target non-negative matrix S can be approximated with the multiplication between a non-negative template matrix W and a non-negative activation matrix H . When applied to audio, S is usually a time-frequency representation of the audio recording, W is the template matrix representing each audio source, and H represents the instants in which each source is active. As such, the rows of W represent frequency bins, the columns of W and the rows of H refer to sound sources, and the columns of H are time frames. The W and H matrices are first initialized with some initial values and then updated until some loss function comparing S and $W \times H$ is minimized. The proposed method for NMF is shown in figure 1 and is similar to previous works [5], [10]. More details are provided in the accompanying website.

Once the NMF algorithm is finished, we use the original perfectly aligned activation matrix to select the region of a note in H and W to obtain its approximated spectrogram separated from the rest of the recording. We consider the first 30 frames (690 ms) of each note, padding with 0 if the note is shorter. We finally compute the first 13 MFCC features in each column of the spectrogram using Essentia.

V. NEURAL NETWORK MODELS

For every function estimation, we use Convolutional Neural Networks (CNN) with skip connections similarly to

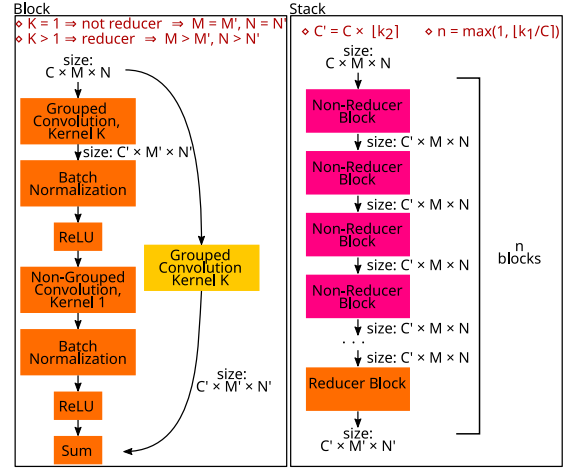


Figure 2. Architecture of the Residual blocks and stacks networks used in this work. $\lfloor \cdot \rfloor$ denotes the rounding operation.

ResNet [16]. A schematic representation of the proposed model building blocks is shown in Figure 2.

In ResNet, a building block is defined so that the output can have the same size as the input (“not reducer” block) or can be reduced (“reducer” block); in both cases, the output of each block is summed to the input to prevent the vanishing gradients phenomenon and other degradation problems connected with the increase of the network complexity [16]. Since they can maintain the output size equal to the input, a virtually infinite number of blocks can be put one after the other, and multiple stacks of blocks can be concatenated to create arbitrarily large and complex networks without depending on the input size.

In the proposed model, each block consists of the following elements:

- a grouped convolutional layer with kernel size K ; if the block is a not-reducer, a padding is used;
- a batch-normalization layer;
- a ReLU non-linear activation;
- a non-grouped convolutional layer with kernel size 1 – corresponding to a linear combination of each data entry across channels;
- another batch-normalization layer;
- a final ReLU activation.

Furthermore, each block sums its output to the input processed with a grouped convolutional layer having kernel size 1 if the block is a not reducer and K otherwise. Figure 2 better depicts the building of a single block.

Multiple blocks can be put one after the other forming a stack. In each stack, the first block changes the number of channels, while the rest keeps it constant. Moreover, all blocks in a stack are not reducers except the last one. As such, each stack can increase or decrease the number of channels in the data representation and at the same time it decreases the size of the data with only one convolution. Figure 2 represents a stack.

In order to control the complexity of the network, we designed a family of CNNs that vary the ratio between the

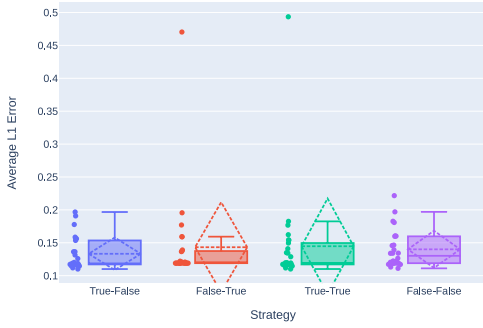


Figure 3. Comparison between the 4 proposed strategies. **False-False** strategy corresponds to the traditional context-unaware transcription function. The dotted rhombus represents average and standard deviation. The continuous line represents the median and box-plot.

number of blocks and the number of channels in each stack based on two parameters k_1 and k_2 . By setting k_1 and k_2 , one may find Residual CNNs that approximate various types of functions. Specifically, k_1 is inversely proportional to k_2 while k_1 is related to the number of blocks and k_2 is connected with the number of channels – see Fig. 2. In our experiments, we manually found that $k_1 = 4$ comprises an effective parameter and observed the way the models perform when k_2 changes. Following this algorithm, multiple stacks were concatenated until the output size has at least one dimension $< k_0$, where k_0 is the kernel size, which is fixed across the stacks.

We use multiple of such CNNs in each model to estimate encoder and performer functions and an additional one for the context classifier. After the stacks, a further convolutional layer followed by batch normalization and ReLU is added aiming at reducing the data size to 1 and at compressing all existing information into the channel dimension; in the performer and context classifier, this last block also takes care of reducing the number of channels to the expected output dimension, i.e. 1 for the velocity and 6 for the context classifier. Finally, we apply a linear transformation using a grouped convolution and activation block with kernel size 1; the last activation is a ReLU in the encoder, a Sigmoid in the performers, and a SoftMax in the context classifier.

The considered hyper-parameters were 4:

- 1) the kernel size in the encoder (values: 3, 5)
- 2) the kernel size in the performer (values: 3, 5)
- 3) the k_2 parameter in the encoder (values: 1, 2, 3)
- 4) the k_2 parameter in the performer (values: 1, 2, 4)

The context classifier branch is built with the same performer kernel; however, due to the higher computational complexity needed for classifying 6 labels, $\{k_1, k_2\}$ were multiplied by 1.25 – i.e. $k_1 = 5$ and $[k_2] \in \{1, 3, 5\}$.

VI. TRAINING

The training datasets include millions of music notes. To make the problem computationally accessible, we use only 0.1% of the available data with a batch size of 10, resulting in 703 batches (7030 notes). Subsampling was performed with a uniform distribution and was repeated on all 6 contexts and splits (train, validation, and test sets). Overall, the training set

Table II

WIN ANALYSIS. THE TABLE MUST BE RIDDEN AS: “STRATEGY AT ROW x IS BETTER THAN STRATEGY AT COLUMN y IN n HYPER-PARAMETER CONFIGURATIONS”

	False-False	True-False	False-True	True-True	All
False-False	-	2	12	3	1
True-False	24	-	19	11	11
False-True	14	7	-	6	5
True-True	23	12	20	-	12

is made of 566 batches, the validation counted 63 batches, and the test set is composed of 74 batches.

Training is performed using Adadelta [17] optimizer with initial learning rate set according to an existing algorithm designed to find its optimal value based on repeated small experiments with increasing learning rates [18]. When the algorithm fails, the initial learning rate is automatically set to $1e-5$. The loss function for the performers is the L1 error, while for the context classifier we use the Cross-Entropy loss. When the context classifier is used, we treat the problem from a multi-task perspective. For this reason, we sum the two losses and use the recently proposed RotoGrad algorithm [19] to stabilize the gradients. Moreover, when using multiple performers, to speed up the training process, we load data so that each batch contains notes related to only one context at a time and we cycle across context so that all of them are equally represented. However, this strategy leads to unstable losses both in training and in validation, making it hard to understand when the model is actually overfitting. As such, we imposed an early-stop procedure with a patience of 20 by observing the Exponential Moving Average of the validation loss on a window of 15 epochs.

VII. RESULTS

The results we obtained are shown in Figure 3 and 4. We computed the average L1 error for velocity estimation in each tested hyper-parameter set, discarding those configurations that generated models exceeding GPU or even CPU RAM or that returned invalid losses. Overall, we considered 26 hyper-parameter sets corresponding to 104 runs. Moreover, to reduce the computational burden, we stopped each training at the 40th epoch, in case the training procedure was not terminated by the early-stopping criterion.

For evaluating the statistical significance of the results in Figure 3, we applied the Shapiro-Wilk normality test to each strategy distribution and then Kruskal-Wallis and Wilcoxon signed-rank test for post-hoc analysis. We found that all analyzed distributions rejected the null hypothesis of normality tests with $p < 4e-3$, meaning that the distributions are not normal. We found no significant difference according to the omnibus Kruskal-Wallis test ($p = 1.74e-1$). However, we also computed the Wilcoxon p-values using the Bonferroni-Holm correction and found a statistically significant difference with confidence of 95% only between True-False and False-False, True-True and False-False. Note that the $p > 0.05$ found with the Kruskal-Wallis test is coherent with the pairwise significance found using the corrected Wilcoxon test [20], [21].

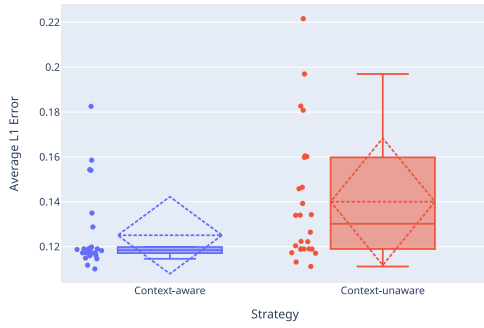


Figure 4. Comparison between the best context-aware strategy and the traditional context-unaware transcription in each hyper-parameter point. The dotted rhombus represents average and standard deviation. The continuous line represents the median and box-plot.

Given the statistical analysis, we argue that $R > 0$ for the True-True and True-False strategies. To further assess such conclusions, we also computed the number of hyper-parameter sets won by each strategy. Table II shows this analysis and highlights how in only 1 configuration the best training strategy was False-False.

However, no optimal strategy was found. Indeed, considering True-False, False-True, and True-True, there is no agreement about which one is the most effective method. To obtain a deeper understanding of the problem, we tried to check what would happen in case an oracle could indicate the optimal strategy depending on the model shape. Results were highly statistically significant ($p = 6e-5$) and showed far improved results when one of the proposed context-aware strategy was used – see Figure 4. This result highlights how, in theory, the benefit coming from context-aware AMT can be definitely larger than 0.

VIII. CONCLUSIONS

In this paper, we proposed an extensible framework to deepen the understanding of acoustical factors on music performance analysis from the perspective of AMT. Future works could also estimate non-MIDI parameters that are relevant for the timbre realization of pianists [9]. Another attractive addition would be the note offset precise inference based on the hammer second and third impulsive sound; given the low accuracy of the note offset inference in state-of-the-art AMT models, such an addition could be useful for precisely defining the performer interpretation. A third addition could be performer-specific adaptation functions, as suggested in previous experiments [22]. Finally, an important parameter that we plan to focus in next works is the pedaling level estimation.

In this work, we extensively evaluated 4 different strategies for velocity estimation of single notes. We demonstrated that considering context-aware strategies consistently improves model performance. However, no context-aware strategy was found to outperform the rest; it was shown that they complement each other.

REFERENCES

- [1] E. Benetos, S. Dixon, Z. Duan, and S. Ewert, “Automatic music transcription: An overview,” *IEEE Sig. Process. Mag.*, vol. 36, no. 1, pp. 20–30, 2019.
- [2] C. Hawthorne, E. Elsen, J. Song, A. Roberts, I. Simon, C. Raffel, J. Engel, S. Oore, and D. Eck, “Onsets and frames: Dual-objective piano transcription,” *Proc. 19th ISMIR*, pp. 50–57, 2018.
- [3] Q. Kong, B. Li, X. Song, Y. Wan, and Y. Wang, “High-resolution piano transcription with pedals by regressing onset and offset times,” *IEEE/ACM TASLP*, pp. 1–1, 2021.
- [4] Y. Yan, F. Cwilkowitz, and Z. Duan, “Skipping the frame-level: Event-based piano transcription with neural semi-crfs,” in *NeurIPS*, 2021.
- [5] F. Simonetta, F. Avanzini, and S. Ntalampiras, “A perceptual measure for evaluating the resynthesis of automatic music transcriptions,” *Multimed. Tools Appl.*, 2022. Accepted.
- [6] M. Xu, Z. Wang, and G. G. Xia, “Transferring piano performance control across environments,” in *ICASSP 2019*, pp. 221–225, 2019.
- [7] F. Simonetta, S. Ntalampiras, and F. Avanzini, “Audio-to-score alignment using deep automatic music transcription,” in *Proc. of the IEEE MMSP 2021*, 2021.
- [8] D. D. Lee and H. S. Seung, “Algorithms for non-negative matrix factorization,” *Adv. Neur. Inf. Process. Syst. 13*, pp. 556–562, 2001.
- [9] M. Bernays and C. Traube, “Investigating pianists individuality in the performance of five timbral nuances through patterns of articulation, touch, dynamics, and pedaling,” *Front. Psychol.*, vol. 5, 2014.
- [10] D. Jeong, T. Kwon, and J. Nam, “Note-intensity estimation of piano recordings using coarsely aligned midi score,” *J. Audio Eng. Soc.*, vol. 68, 2020.
- [11] F. Alías, J. Socoró, and X. Sevillano, “A review of physical and perceptual feature extraction techniques for speech, music and environmental sounds,” *Appl. Sci.*, vol. 6, no. 5, p. 143, 2016.
- [12] C. Hawthorne, A. Stasyuk, A. Roberts, I. Simon, C.-z. A. Huang, S. Dieleman, E. Elsen, J. H. Engel, and D. Eck, “Enabling factorized piano music modeling and generation with the maestro dataset,” *Proc. Int. Conf. on Learn. Represent.*, 2019.
- [13] F. Simonetta, S. Ntalampiras, and F. Avanzini, “Asmd: an automatic framework for compiling multimodal datasets,” *Proc. 17th Sound Music. Comput. Conf.*, 2020.
- [14] E. Benetos, A. Klapuri, and S. Dixon, “Score-informed transcription for automatic piano tutoring,” in *EUSIPCO*, pp. 2153–2157, 2012.
- [15] S. Wang, S. Ewert, and S. Dixon, “Identifying missing and extra notes in piano recordings using score-informed dictionary learning,” *IEEE/ACM Trans. on Audio, Speech, Lang. Process.*, vol. 25, no. 10, pp. 1877–1889, 2017.
- [16] K. He, X. Zhang, S. Ren, and J. Sun, “Deep residual learning for image recognition,” *2016 IEEE CVPR*, pp. 770–778, 2016.
- [17] M. D. Zeiler, “Adadelta: An adaptive learning rate method,” *arXiv preprint arXiv:1212.5701*, 2012.
- [18] L. N. Smith, “Cyclical learning rates for training neural networks,” in *2017 IEEE WACV*, pp. 464–472, 2017.
- [19] A. Javaloy and I. Valera, “Rotograd: Dynamic gradient homogenization for multi-task learning,” 2021.
- [20] J. Hsu, *Multiple Comparisons*. Chapman and Hall/CRC, 1996.
- [21] S. E. Maxwell, H. D. Delaney, and K. Kelley, *Designing Experiments and Analyzing Data*. Routledge, 2017.
- [22] Z. S. Kalkandjiev and S. Weinzierl, “The influence of room acoustics on solo music performance: An experimental study,” *Psychomusicology: Music. Mind, Brain*, vol. 25, no. 3, pp. 195–207, 2015.